Rheology of gelling polymers in the Zimm model

ARTICLE *in* THE JOURNAL OF CHEMICAL PHYSICS · FEBRUARY 2005

Impact Factor: 2.95 · DOI: 10.1063/1.1813433 · Source: PubMed

3 AUTHORS, INCLUDING:

Henning Löwe
WSL Institute for Snow and Avalanche Resea…
25 PUBLICATIONS **403** CITATIONS
SEE PROFILE

Annette Zippelius
Georg-August-Universität Göttingen
164 PUBLICATIONS **3,534** CITATIONS
SEE PROFILE

Rheology of gelling polymers in the Zimm model

Henning Löwe,* Peter Müller,† and Annette Zippelius‡
Institut für Theoretische Physik, Georg-August-Universität, D–37077 Göttingen, Germany
(Dated: February 2, 2008)

In order to study rheological properties of gelling systems in dilute solution, we investigate the viscosity and the normal stresses in the Zimm model for randomly crosslinked monomers. The distribution of cluster topologies and sizes is assumed to be given either by Erdős-Rényi random graphs or three-dimensional bond percolation. Within this model the critical behaviour of the viscosity and of the first normal stress coefficient is determined by the power-law scaling of their averages over clusters of a given size n with n. We investigate these Mark–Houwink like scaling relations numerically and conclude that the scaling exponents are independent of the hydrodynamic interaction strength. The numerically determined exponents agree well with experimental data for branched polymers. However, we show that this traditional model of polymer physics is not able to yield a critical divergence at the gel point of the viscosity for a polydisperse dilute solution of gelation clusters. A generally accepted scaling relation for the Zimm exponent of the viscosity is thereby disproved.

I. INTRODUCTION

The influence of hydrodynamic interactions on critical rheological properties of gelling polymeric systems has been discussed controversely for many decades. In particular, the experimental values for the exponent k, which governs the divergence of the shear viscosity $\eta \propto \varepsilon^{-k}$ with vanishing distance ε to the critical gel point, scatter considerably, see Table I for some examples. In order to interpret the wide scatter of the data, they are often related to either Zimm or Rouse dynamics, depending on whether hydrodynamic interactions are believed to be relevant or not. In this paper we intend to elaborate on the validity of this interpretation, so let us be precise with the labels. By definition, the *Rouse* model[1] neglects both hydrodynamic and excluded-volume interactions. Its straightforward generalization from linear polymers to a gelling melt of randomly crosslinked monomers provides a microscopic framework, within which one can derive an exact scaling relation for the viscosity exponent.[2,3,4,5,6] The *Zimm* model,[7] by definition, takes hydrodynamic interactions into account on a preaveraged level, but still neglects excluded-volume interactions. We are not aware of a microscopic approach based on the Zimm model which allows for an exact analytic computation of the viscosity exponent for a gelling polymeric solution. Other models for gelling polymers, which go beyond the Rouse or Zimm model by incorporating excluded-volume effects or fluctuating hydrodynamic interactions, are conjectured to belong to *different* universality classes and will not be considered here.

Scaling theory[16,17,18] has proven to be a powerful tool to describe the properties of polymeric systems. The relaxation time t_n of a typical cluster of n monomers (henceforth n will be referred to as the *size* of the cluster) is estimated to be $t_n \sim R_n^2/D_n$, where R_n is the radius of gyration and D_n the diffusion constant of the cluster. The scaling $R_n \sim n^{1/d_f}$ of the radius of gyration of a cluster with size n is determined by the Hausdorff fractal dimension d_f. The diffusion constant is assumed to scale like $D_n \sim 1/R_n$ in the Zimm model. This assumption is based on the Stokes Einstein relation which is valid for linear polymers and still holds for the diffusion of fractal polymer clusters in the Zimm model.[19] The average contribution of clusters of size n to the viscosity is then given by $\eta_n \sim t_n/n$. This implies the scaling[16,17,18]

$$\eta_n \sim n^{b_\eta}, \qquad b_\eta = d/d_f - 1 \tag{1}$$

where d is the spatial dimension. With an underlying distribution of cluster sizes, which is widely believed to follow the scaling laws of percolation, this gives rise to the exponent $k = (1 - \tau + d/d_f)/\sigma$ for the averaged viscosity in terms of the static percolation exponents.

k	0.2	0.79	0.82	0.95	1.27	1.36	> 1.4	6.1
Ref.	8	9	10	11	12	13	14	15

TABLE I: Experimental data for the critical exponent k of the viscosity at the gelation transition.

Beside critical properties, recent publications aim at the dynamics of single clusters with particular topologies within the Zimm model. Refs. 20 and 21 consider the Zimm dynamics of star-shaped clusters and dendrimers, and Ref. 22 analyses the relaxation behaviour of fractal (Sierpinski-type) clusters in the Zimm model. The latter authors mention the possibility of non-universal behaviour. The question of non-universality is also raised from computer simulations[23] of gelling liquids under the influence of solvent particles.

In this paper we investigate the viscosity and the normal stresses in the Zimm model for randomly crosslinked monomers. The distribution of cluster topologies and sizes is assumed to be given either by Erdős–Rényi random graphs or three-dimensional bond percolation. The details of the model are described in Section II. Within this model, the critical behaviour of the viscosity η and of the first normal stress coefficient $\Psi^{(1)}$ is determined by the scaling with n of the partial averages $\eta_n \sim n^{b_\eta}$, respectively $\Psi_n^{(1)} \sim n^{b_\Psi}$, over clusters of size n (Section III). In Section IV we investigate these Mark–Houwink like scaling relations numerically for different strengths of the hydrodynamic coupling constant. We conclude in Section V that (i) these scaling relations are governed by universal exponents b_η and b_Ψ. This conclusion is substantiated by comparing our results to those for ring polymers in the Zimm model, which are known to exhibit universal behaviour. (ii) We find that the scaling relation (1) does not agree with our numerical data and, hence, does not describe

the viscosity in the Zimm model for randomly crosslinked monomers.

II. DYNAMIC MODEL AND ITS SOLUTION

A. Hydrodynamic Interactions

We consider N point-like monomers, which are characterized by their time-dependent position vectors $\mathbf{R}_i(t)$, $i = 1,\ldots,N$, in three-dimensional Euclidean space. Permanently formed crosslinks constrain M randomly chosen pairs of particles (i_e, j_e), $e = 1,\ldots,M$. We study the dynamics of crosslinked monomers in the presence of a solvent fluid, giving rise to hydrodynamic interactions between the monomers. Purely relaxational dynamics in an incompressible fluid subjected to an external space- and time-dependent flow $\mathbf{v}(\mathbf{r},t)$ is described by the equation of motion[24,25]

$$\frac{d}{dt}\mathbf{R}_i(t) - \mathbf{v}(\mathbf{R}_i(t),t) = \sum_{j=1}^{N} \mathsf{H}_{i,j}\big(\mathbf{R}_i(t) - \mathbf{R}_j(t)\big)\Big(-\frac{\partial V}{\partial \mathbf{R}_j(t)}\Big) + \mathbf{f}_i(\mathbf{R}_i(t),t)\,. \tag{2}$$

Here, crosslinks are modelled by Hookean springs in the potential energy

$$V := \frac{3}{2a^2}\sum_{e=1}^{M}\big(\mathbf{R}_{i_e} - \mathbf{R}_{j_e}\big)^2 =: \frac{3}{2a^2}\sum_{i,j=1}^{N}\mathbf{R}_i\cdot\Gamma_{i,j}\,\mathbf{R}_j\,, \tag{3}$$

where the length $a > 0$ plays the role of an inverse crosslink strength and physical units have been chosen such that $k_{\mathrm{B}}T = 1$. A given crosslink configuration $\mathcal{G} = \{i_e, j_e\}_{e=1}^{M}$ is specified by its $N\times N$-connectivity matrix Γ. Moreover, we impose a simple shear flow

$$\mathbf{v}(\mathbf{r},t) := \begin{pmatrix} 0 & \dot\gamma(t) & 0\\ 0 & 0 & 0\\ 0 & 0 & 0\end{pmatrix}\mathbf{r}, \tag{4}$$

which is characterized by its time-dependent shear rate $\dot\gamma(t)$. The mobility matrix is given by

$$\mathsf{H}_{i,j}(\mathbf{r}) := \delta_{i,j}\,\frac{1}{\zeta}\,\mathbf{1} + (1-\delta_{i,j})\,\frac{1}{8\pi\eta_s|\mathbf{r}|}\,\Big(\mathbf{1} + \frac{\mathbf{r}\mathbf{r}^\dagger}{|\mathbf{r}|^2}\Big). \tag{5}$$

The diagonal term in (5) accounts for a frictional force with friction constant ζ that acts when a monomer moves relative to the externally imposed flow field (4). The non-diagonal term reflects the influence of the motion of monomer j on the solvent at the position of monomer i and is given by the Oseen tensor.[26,27] Here η_s denotes the solvent viscosity, $\delta_{i,j}$ the Kronecker symbol, $\mathbf{1}$ the three-dimensional unit matrix and the dagger indicates the transposition of a vector. Rouse dynamics is recovered, if the non-diagonal terms $i \neq j$ of the mobility matrix are neglected. The Gaussian thermal-noise force fields $\mathbf{f}_i(\mathbf{r},t)$ in (2) have zero mean and covariance

$$\overline{\mathbf{f}_i(\mathbf{r},t)\,\mathbf{f}_j^\dagger(\mathbf{r}',t')} = 2\,\mathsf{H}_{i,j}(\mathbf{r}-\mathbf{r}')\,\delta(t-t')\,. \tag{6}$$

Here δ stands for the Dirac-delta function and the overbar indicates the Gaussian average over all realizations of $\mathbf{f}$.

In order to determine the model completely, it only remains to specify the probability distribution of the crosslink configurations. We shall discuss two different types of probability distributions: (i) crosslinks are chosen independently with equal probability for every pair of monomers, corresponding to Erdős–Rényi random graphs,[28] and (ii) a distribution of crosslinks, which generates clusters amenable to the scaling description of finite-dimensional percolation.[29] The precise characterization of these distributions is given below.

B. Preaveraging Approximation

The equation of motion (2) is nonlinear due to the nonlinear dependence of the mobility on the particles' positions. A simple but uncontrolled approximation is the so-called preaveraging approximation that was first introduced by Kirkwood and Riseman[27] and Zimm.[7] In this approximation the mobility matrix (5) is replaced by its expectation value $\langle\mathsf{H}_{i,j}\rangle_{\mathrm{eq}}$, which is computed with respect to the equilibrium distribution, i.e. the Boltzmann weight $\sim e^{-V}$. Due to rotational invariance of the potential (3), the averaged mobility matrix is a multiple of the identity matrix $\langle\mathsf{H}_{i,j}(\mathbf{R}_i-\mathbf{R}_j)\rangle_{\mathrm{eq}} = \mathsf{H}^{\mathrm{eq}}_{i,j}\,\mathbf{1}$, where

$$\mathsf{H}^{\mathrm{eq}}_{i,j} := \delta_{i,j}\,\frac{1}{\zeta} + (1-\delta_{i,j})\,\frac{1}{6\pi\eta_s}\,\Big\langle\frac{1}{|\mathbf{R}_i-\mathbf{R}_j|}\Big\rangle_{\mathrm{eq}}\,. \tag{7}$$

In the computation of (7), care has to be taken of the zero eigenvalues of the connectivity matrix, corresponding to the translation of whole clusters. To this end we regularize the potential (3) by adding a confining term $3\omega/(2a^2)\sum_{i=1}^{N}\mathbf{R}_i\cdot\mathbf{R}_i$ and letting $\omega > 0$ tend to zero subsequently. The average in (7) is conveniently performed via the Fourier representation of $1/|\mathbf{r}|$, and the result

$$\Big\langle\frac{1}{|\mathbf{R}_i-\mathbf{R}_j|}\Big\rangle_{\mathrm{eq}} = \frac{1}{a}\sqrt{\frac{6}{\pi}}\,\lim_{\omega\downarrow 0}\Big([\mathsf{G}(\omega)]_{i,i} + [\mathsf{G}(\omega)]_{j,j} - 2[\mathsf{G}(\omega)]_{i,j}\Big)^{-1/2} \tag{8}$$

involves the resolvent $\mathsf{G}(\omega) := (\Gamma+\omega 1)^{-1}$ of Γ. The limit $\omega\downarrow 0$ is taken by expanding the resolvent $\mathsf{G}(\omega) = \mathsf{E}_0/\omega + \mathsf{Z} + \mathcal{O}(\omega)$ in terms of ω. Here $\mathsf{Z} := (1-\mathsf{E}_0)/\Gamma$ is the Moore–Penrose inverse[30] of the connectivity matrix, *i.e.* the inverse of Γ restricted to the subspace of non-zero eigenvalues. Moreover, 1 denotes the $N\times N$-unit matrix and E_0 the projector on the nullspace of Γ, which is spanned by the vectors that are constant when restricted to any one cluster of crosslinked

monomers. More precisely, the matrix element $[\mathsf{E}_0]_{i,j}$ is given by the inverse number of monomers of the cluster if i and j are in the same cluster and zero otherwise (cf. Sec. II.D in Ref. 3 for details). Hence, the right-hand side of (8) vanishes for $\omega \downarrow 0$ whenever i and j belong to different clusters. Consequently, the preaveraged mobility matrix $\mathsf{H}^{\rm eq}$ shows correlations of different particles only if these particles are in the same cluster, in other words it is block-diagonal and within one block given by

$$\mathsf{H}^{\rm eq}_{i,j} = \frac{1}{\zeta}\,\Big[\delta_{i,j} + (1-\delta_{i,j})\,h\left(\kappa^2\,\pi/\mathcal{R}_{i,j}\right)\Big]\,. \tag{9}$$

For convenience we introduced the function $h(x) = \sqrt{x/\pi}$ and the quantity $\mathcal{R}_{i,j} := \mathsf{Z}_{i,i} + \mathsf{Z}_{j,j} - 2\mathsf{Z}_{i,j}$, which can be interpreted as the resistance between nodes i and j in a corresponding electrical resistor network.[31] The parameter $\kappa := \sqrt{6/\pi}\,\zeta/(6\pi\eta_s a)$ plays the role of the coupling constant of the hydrodynamic interaction. Note that this definition of κ differs from that of other authors by a factor of $\sqrt{2}$,[32] respectively $\sqrt{6}/\pi$.[22] Formally setting $\kappa = 0$ in (9) yields $\mathsf{H}^{\rm eq}_{i,j} = \zeta^{-1}\delta_{i,j}$, and the Zimm model for gelation reduces to the Rouse model for gelation.[2,3,4,5,6,33] It is well known that the Oseen tensor does not give rise to a positive-definite mobility matrix for all possible spatial configurations of monomers. This defect is cured if the Rotne–Prager–Yamakawa tensor[34,35] is used instead. Again, the preaveraging procedure is done with a confining potential which is switched off afterwards. The function h is then given by[36]

$$h(x) = \mathrm{erf}(\sqrt{x}) - \frac{1}{\sqrt{\pi}}\frac{1-\exp(-x)}{\sqrt{x}}. \tag{10}$$

It involves the error function $\mathrm{erf}(x)$ and recovers the form of the preaveraged Oseen-Tensor asymptotically as $x \downarrow 0$. As a result of preaveraging we obtain the *Zimm model for crosslinked monomers in solution*

$$\frac{d}{dt}\mathbf{R}_i(t) - \mathbf{v}(\mathbf{R}_i(t),t) = -\sum_{j=1}^{N}\mathsf{H}^{\rm eq}_{i,j}\,\frac{\partial V}{\partial \mathbf{R}_j(t)} + \boldsymbol{\xi}_i(t)\,. \tag{11}$$

Here, the covariance of the thermal noise is given by

$$\overline{\boldsymbol{\xi}_i(t)\,\boldsymbol{\xi}_j^{\dagger}(t')} = 2\,\mathsf{H}^{\rm eq}_{i,j}\,\delta(t-t')\mathbf{1}\,. \tag{12}$$

Since both the connectivity matrix Γ and the preaveraged mobility matrix $\mathsf{H}^{\rm eq}$ are block-diagonal, it follows that clusters move *independently* of each other in this model.

C. Formal Solution

The Zimm equation (11) is linear, hence it can be solved exactly. This is most conveniently done by introducing new coordinates $\widetilde{\mathbf{R}}_i(t)$ through the coordinate transformation

$$\mathbf{R}_i(t) =: \sum_{j=1}^{N}\Big[\left(\mathsf{H}^{\rm eq}\right)^{1/2}\Big]_{i,j}\,\widetilde{\mathbf{R}}_j(t)\,. \tag{13}$$

The resulting equation of motion for $\widetilde{\mathbf{R}}_i(t)$ coincides with that of the Rouse model for crosslinked monomers,[2,3,4,5,6,33] if one replaces the connectivity matrix Γ by

$$\widetilde{\Gamma} := \left(\mathsf{H}^{\rm eq}\right)^{1/2}\Gamma\,\left(\mathsf{H}^{\rm eq}\right)^{1/2} \tag{14}$$

in the latter. Different coordinate transformations are commonly used to establish this formal relation between the two models. We prefer (13), because then the transformed equation of motion involves the *symmetric* matrix (14). The resulting monomer trajectories for (transformed) initial data $\widetilde{\mathbf{R}}_i(t_0)$ are therefore given by

$$\widetilde{\mathbf{R}}_i(t) = \sum_{j=1}^{N}\Big\{\widetilde{\mathsf{U}}_{i,j}(t-t_0)\,\mathbf{T}(t,t_0)\,\widetilde{\mathbf{R}}_j(t_0) + \int_{t_0}^{t} dt'\,\widetilde{\mathsf{U}}_{i,j}(t-t')\,\mathbf{T}(t,t')\,\widetilde{\boldsymbol{\xi}}_j(t')\Big\}\,, \tag{15}$$

as follows e.g. from Sec. II.C in Ref. 3. The solution (15) is expressed in terms of the transformed thermal noise with zero mean and covariance

$$\overline{\widetilde{\boldsymbol{\xi}}_i(t)\,\widetilde{\boldsymbol{\xi}}_j^{\dagger}(t')} = 2\,\delta_{i,j}\,\delta(t-t')\mathbf{1}\,, \tag{16}$$

and the time evolution in the simple shear flow (4) is characterized by the $N\times N$-matrix

$$\widetilde{\mathsf{U}}(t) := \exp\{-3\,t\,\widetilde{\Gamma}/a^2\} \tag{17}$$

and the 3×3-matrix

$$\mathbf{T}(t,t') := \begin{pmatrix} 1 & \int_{t'}^{t} ds\,\dot\gamma(s) & 0\\ & 1 & 0\\ 0 & 0 & 1\end{pmatrix}\,. \tag{18}$$

Finally, the solution of the Zimm equation (11) is obtained by inserting (15) in (13).

III. OBSERVABLES

A. Shear Stress

We shall focus on the viscosity η and the first and second normal stress coefficients $\Psi^{(1)}$ and $\Psi^{(2)}$, respectively. Therefore we need to compute the intrinsic shear stress $\boldsymbol{\sigma}(t)$ as a function of the shear rate $\dot\gamma(t)$. Following Chap. 3 in Ref. 24 or Chap. 16.3 in Ref. 25, we express the shear stress in terms of the force per unit area exerted by the polymers

$$\boldsymbol{\sigma}(t) = \lim_{t_0\to-\infty} -\frac{\rho_0}{N}\sum_{i=1}^{N}\overline{\mathbf{F}_i(t)\mathbf{R}_i^{\dagger}(t)}. \tag{19}$$

Here, $\mathbf{R}_i(t)$ is the solution of the equation of motion (11) with some initial condition $\mathbf{R}_i(t_0)$ at time t_0 in the distant past (so that all transient effects stemming from the initial condition

have died out). Moreover, ρ_0 stands for the monomer concentration and $\mathbf{F}_i(t) := -\partial V/\partial \mathbf{R}_i(t)$ is the net spring force acting on monomer i at time t. Using the transformation (13) and the solution (15), it is readily shown[3,4] that the stress tensor (19) is given by

$$\boldsymbol{\sigma}(t) = \chi(0)\,\mathbf{1} + \int_{-\infty}^{t} dt'\; \chi(t-t')\,\dot\gamma(t') \times \begin{pmatrix} 2\int_{t'}^{t} ds\,\dot\gamma(s) & 1 & 0 \\ 1 & 0 & 0 \\ 0 & 0 & 0 \end{pmatrix} \qquad (20)$$

for arbitrary strengths of the shear rate $\dot\gamma(t)$. Here, we have defined the stress-relaxation function

$$\chi(t) := \frac{\rho_0}{N}\,\mathrm{Tr}\left[(1-\widetilde{\mathsf{E}}_0)\exp\left(-\frac{6t}{a^2}\,\widetilde\Gamma\right)\right] \qquad (21)$$

as a trace over the subspace of non-zero eigenvalues of $\widetilde\Gamma$.

For a time-independent shear rate $\dot\gamma$, the shear stress (20) is also independent of time. The (intrinsic zero-shear) viscosity η is then related to shear stress via

$$\eta := \frac{\sigma_{x,y}}{\dot\gamma\rho_0} \qquad (22)$$

and the normal stress coefficients are defined by

$$\Psi^{(1)} := \frac{\sigma_{x,x}-\sigma_{y,y}}{\dot\gamma^2\rho_0}\,, \qquad \Psi^{(2)} := \frac{\sigma_{y,y}-\sigma_{z,z}}{\dot\gamma^2\rho_0}\,, \qquad (23)$$

respectively. Hence, the viscosity (22) is given by

$$\eta(\mathcal{G}) = \frac{1}{\rho_0}\int_0^\infty dt\,\chi(t) = \frac{a^2}{3}\,\frac{1}{2N}\,\mathrm{Tr}\left[\frac{1-\widetilde{\mathsf{E}}_0}{\widetilde\Gamma(\mathcal{G})}\right] \qquad (24)$$

for a fixed realization $\mathcal{G}$ of crosslinks. It is determined by the trace of the Moore–Penrose inverse of $\widetilde\Gamma(\mathcal{G})$. According to (20) and (23), the second normal stress coefficient $\Psi^{(2)}$ vanishes always, whereas

$$\Psi^{(1)}(\mathcal{G}) = \frac{2}{\rho_0}\int_0^\infty dt\,t\,\chi(t) = \left(\frac{a^2}{3}\right)^2\,\frac{1}{2N}\,\mathrm{Tr}\left[\frac{1-\widetilde{\mathsf{E}}_0}{\big(\widetilde\Gamma(\mathcal{G})\big)^2}\right]. \qquad (25)$$

Again, we have made explicit the dependence on $\mathcal{G}$ in (25). This will be convenient for computing the average over all crosslink realizations in the next subsection.

B. Disorder Average and Critical Behaviour

Each crosslink realization $\mathcal{G}$ defines a random labelled graph on the set of monomers, which can be decomposed into maximal path-wise connected components or clusters

$$\mathcal{G} = \bigcup_{k=1}^{K} \mathcal{N}_k\,. \qquad (26)$$

Here, $\mathcal{N}_k$ denotes the k-th cluster with N_k monomers out of a total of K clusters (all depending on $\mathcal{G}$). We also refer to N_k as the size of the cluster $\mathcal{N}_k$. The associated modified connectivity matrix $\widetilde\Gamma$ from (14) is of block-diagonal form with respect to the clusters. Therefore one can decompose any observable of the type $A(\mathcal{G}) = N^{-1}\mathrm{Tr}\,f(\widetilde\Gamma(\mathcal{G}))$, where f is some function on the reals, into contributions from different clusters according to

$$A(\mathcal{G}) = \sum_{k=1}^{K}\frac{N_k}{N}\,A(\mathcal{N}_k)\,. \qquad (27)$$

Here, we have defined $A(\mathcal{N}_k) := N_k^{-1}\mathrm{Tr}\,f(\widetilde\Gamma(\mathcal{N}_k))$. In particular, (27) holds for the viscosity (24) and for the first normal stress coefficient (25).

In order to compute the average $\langle A\rangle$ of the observable A over all crosslink realizations in the macroscopic limit $M\to\infty$, $N\to\infty$ with fixed crosslink concentration $c := M/N$, we have to specify the statistical ensemble that determines the realizations of crosslinks. Two distributions of crosslinks will be considered. (i) Each pair of monomers is chosen independently with equal probability c/N, corresponding to Erdős–Rényi random graphs, which are known to resemble the critical properties of mean-field percolation.[37] After performing the macroscopic limit, there is no macroscopic cluster for $c < c_{\mathrm{crit}} = 1/2$ and almost all clusters are trees.[28] Furthermore, all n^{n-2} trees of a given size n are equally likely. (ii) Clusters are generated according to three-dimensional continuum percolation, which is closely related to the intuitive picture of gelation, where monomers are more likely to be crosslinked when they are close to each other. Since continuum percolation and lattice percolation are believed to be in the same universality class,[29] we employ the scaling description of the latter. It predicts[29] a cluster-size distribution of the form

$$\tau_n := \left\langle N^{-1}\sum_{k=1}^{K}\delta_{N_k,n}\right\rangle \sim n^{-\tau}\exp\{-n/n^*\} \qquad (28)$$

for $\varepsilon := (c_{\mathrm{crit}}-c) \ll 1$ and $n\to\infty$ with a typical cluster size $n^*(\varepsilon)\sim\varepsilon^{-1/\sigma}$ that diverges as $\varepsilon\to 0$. Here, σ and τ are (static) critical exponents.

For the computation of the average $\langle A\rangle$ over all crosslink realizations $\mathcal{G}$ it is convenient to introduce partial averages

$$\langle A\rangle_n := \tau_n^{-1}\left\langle N^{-1}\sum_{k=1}^{K}\delta_{N_k,n}\,A(\mathcal{N}_k)\right\rangle \qquad (29)$$

of A over all clusters of a given size n. Using (27) and reordering the clusters, one gets the identity

$$\langle A\rangle = \left\langle\sum_{k=1}^{K}\frac{N_k}{N}\,A(\mathcal{N}_k)\right\rangle = \sum_{n=1}^{\infty} n\tau_n\langle A\rangle_n\,, \qquad (30)$$

which is valid in the absence of an infinite cluster. Now suppose one has the scaling

$$A_n := \langle A\rangle_n\big|_{\varepsilon=0} \sim n^b \qquad (31)$$

of the partial average at the critical point as $n \to \infty$. Due to the absence of relevant scales at the critical point, this is quite a natural behaviour. Then, (30) and (28) imply the critical divergence

$$\langle A \rangle \sim \varepsilon^{-u} \quad \text{as} \quad \varepsilon \downarrow 0, \quad \text{with} \quad u = (2 - \tau + b)/\sigma \qquad (32)$$

for the crosslink-averaged observable A, provided that $u > 0$. We will therefore study the scaling

$$\eta_n \sim n^{b_\eta} \quad \text{and} \quad \Psi_n^{(1)} \sim n^{b_\Psi} \qquad (33)$$

as $n \to \infty$ to explore critical rheological behaviour at the gelation transition within the Zimm model.

Formulas like (30) – (33) may also be familiar from scaling theories for gelation. We go beyond such approaches in that we have mapped the dynamical properties of a gelling molecular system to a percolation problem, see e.g. (24) and (25). This mapping has been fully derived within a (semi-) microscopic dynamical model, the Zimm model for randomly crosslinked monomers, and not merely postulated from *ad-hoc* assumptions, as is usually done in scaling theories. In the following section we describe the numerical solution of the percolation problem.

IV. NUMERICAL RESULTS

A. Erdős–Rényi Random Graphs

For numerical purposes it is convenient to compute the eigenvalues of the non-symmetric matrix $\widehat{\Gamma} := \mathsf{H}^{\mathrm{eq}}\Gamma$ rather than those of $\widetilde{\Gamma} = (\mathsf{H}^{\mathrm{eq}})^{1/2}\Gamma(\mathsf{H}^{\mathrm{eq}})^{1/2}$ because this prevents us from computing the expensive square root of H^{eq}. The fact that $\widetilde{\Gamma}$ and $\widehat{\Gamma}$ have the same eigenvalues can easily be proven by observing that if ψ is an eigenvector of $\widetilde{\Gamma}$ with corresponding eigenvalue λ then $(\mathsf{H}^{\mathrm{eq}})^{\pm 1/2}\,\psi$ is a right/left eigenvector of $\widehat{\Gamma}$ with the same eigenvalue λ.

As already mentioned in Sec. III B, the average $\langle \bullet \rangle_n$ extends over all n^{n-2} equally weighted labelled trees of size n in the case of Erdős–Rényi random graphs and, hence, is independent of the crosslink concentration c. Random labelled trees of a given size have been generated via the Prüfer algorithm and handled with the LEDA library.[38] The preaveraged mobility matrix (9) is computed with the function h from (10), corresponding to the Rotne–Prager–Yamakawa tensor. The resistances $\mathcal{R}_{i,j}$ in trees reduce to shortest paths, that is graph distances, which are calculated with the Dijkstra algorithm.[38] The eigenvalues of $\widehat{\Gamma}$ are then computed with the LAPACK library. For suitable, logarithmically equidistant cluster sizes $n \in [2, 4000]$ we average the viscosity and the normal stress coefficient over 50 trees, which turned out to yield an acceptable computer-time/accuracy trade-off. In Figs. 1(a) and (b) we plot η_n and $\Psi_n^{(1)}$ as a function of n on a double-logarithmic scale for different values of the hydrodynamic interaction parameter κ. According to (33) the exponents b_η and b_Ψ are obtained by power law fits in the large n-range, for which we choose the interval $n \in [700, 4000]$, see Fig. 1(c). For the viscosity the exponent decreases from $b_\eta = 0.28$ for $\kappa = 0.05$ to $b_\eta = 0.11$ for $\kappa = 0.3$. The Rouse exponent for $\kappa = 0$ is exactly given by[3] $b_\eta = 1/2$. The exponent b_Ψ of the normal stress coefficient ranges from $b_\Psi = 1.2$ for $\kappa = 0.05$ to $b_\Psi = 0.73$ for $\kappa = 0.25$. The Rouse value for $\kappa = 0$ is exactly given[4] by $b_\Psi = 2$.

B. Three-Dimensional Percolation

For the generation of clusters according to three-dimensional *bond percolation* we apply the Leath Algorithm.[39] It generates a sequence $\{\mathcal{N}_l\}_{l=1}^{L}$ of clusters, in terms of which the disorder average is readily computed via $\langle A \rangle = \lim_{L\to\infty} L^{-1} \sum_{l=1}^{L} A(\mathcal{N}_l)$. This implies $\langle A \rangle_n = \lim_{L\to\infty} \sum_{l=1}^{L} \delta_{N_l,n} A(\mathcal{N}_l) / \sum_{l=1}^{L} \delta_{N_l,n}$ for the average over clusters of size n. The algorithm has been tested by verifying the scaling of the cluster-size distribution τ_n. Second, for small values of n, we compared the number of clusters with known exact values.[40] Third, we verified that the exponent $2/d_f$, which governs the scaling of the squared radius of gyration as a function of cluster size n at the critical point,[29] comes out as $2/2.53$ from the simulation. For each generated cluster the resistances $\mathcal{R}_{i,j}$ are computed from the Moore–Penrose inverse Z of the connectivity matrix $\mathit{\Gamma}$ – see below Eq. (9) – and inserted into (9) with h corresponding to the Rotne–Prager–Yamakawa tensor. The eigenvalues of $\widehat{\Gamma}$ are then computed with the LAPACK library. We were forced to restrict cluster sizes to values $n < 4000$ due to the limited amount of memory, which is required for the generation and diagonalization of the matrix product $\widehat{\Gamma} = \mathsf{H}^{\mathrm{eq}}\Gamma$. Moreover, for calculating disorder averages we restrict the number of realizations pertaining to a given cluster size to a maximum of 50. However, within the present numerical effort this maximum number is not even attained for larger cluster sizes. Therefore the disorder averaged quantities are still subject to fluctuations. In order to obtain smooth curves for η_n and Ψ_n we have also smoothed out the raw data by performing a running average over cluster sizes in the window $[n-5, n+5]$. The thus obtained values for η_n and Ψ_n are plotted in Figs. 1(d) and (e), respectively, as a function of n on a double-logarithmic scale for different values of κ. The exponents b_η and b_Ψ, extracted by fitting the curves in Figs. 1(d) and (e) to a power law in the interval $n \in [800, 4000]$, are shown in Fig. 1(f). The numerical values for b_η are nearly identical to those obtained for Erdős–Rényi random graphs. Again, one observes a decrease from $b_\eta = 0.21$ for $\kappa = 0.05$ to $b_\eta = 0.11$ for $\kappa = 0.3$. The exponent b_Ψ of the normal stress coefficient ranges from $b_\Psi = 1.1$ for $\kappa = 0.05$ to $b_\Psi = 0.78$ for $\kappa = 0.25$. The corresponding Rouse values for $\kappa = 0$ follow from exact analytical arguments[2,3,6] and are given by $b_\eta = (2/d_s) - 1 \approx 1/2$ and $b_\Psi = (4/d_s) - 1 \approx 2$, respectively. Here, $d_s \approx 4/3$ is the spectral dimension of the incipient percolating cluster, whose numerical value is very well approximated by the Alexander–Orbach conjecture.[29]

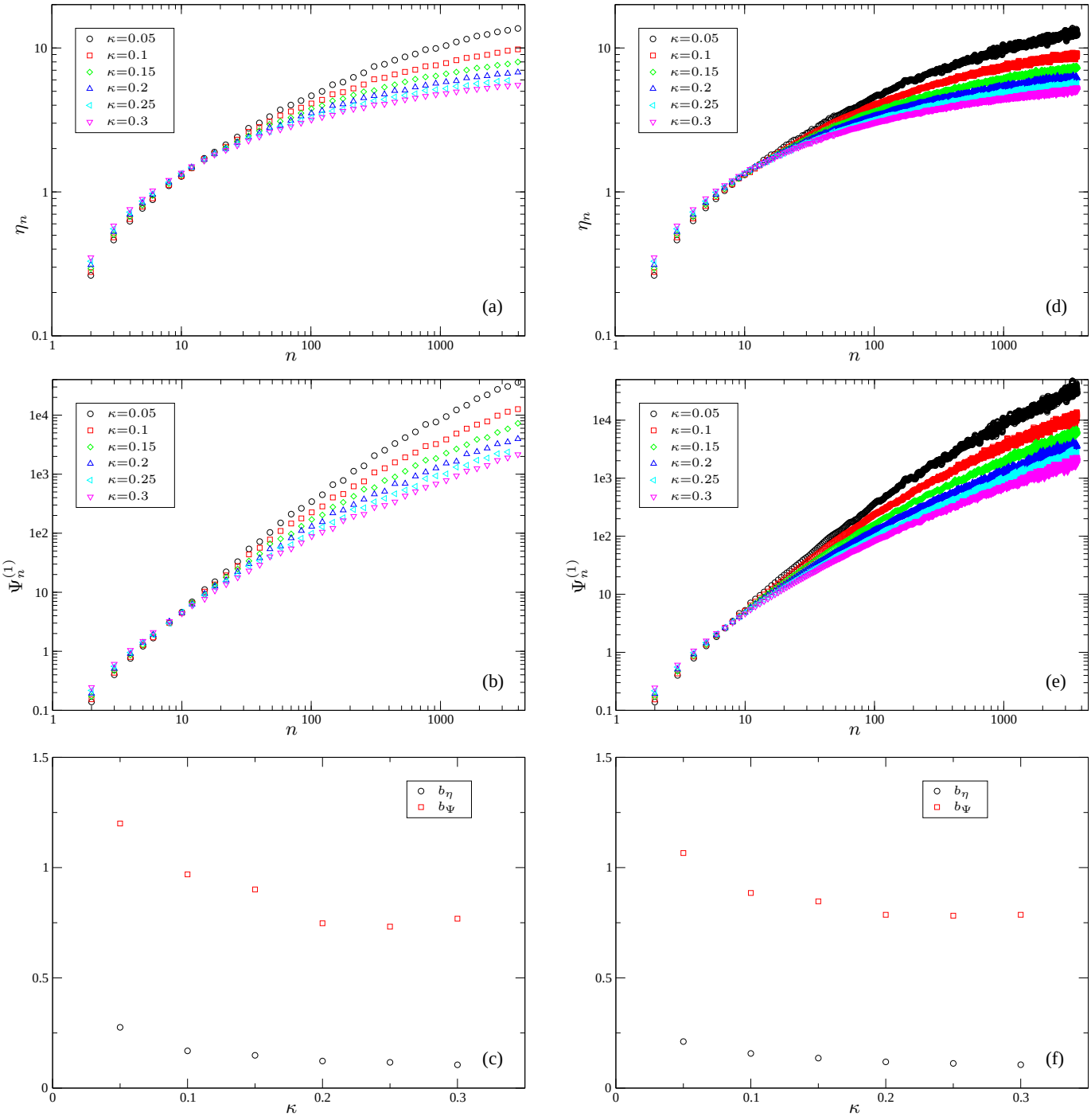

FIG. 1: Numerical data to determine the scaling (33) for random clusters in the case of Erdős–Rényi random graphs (left column) and three-dimensional bond percolation (right column). In each case the averaged viscosity η_n (top) and normal stress coefficient $\Psi_n^{(1)}$ (middle) are plotted for different strengths of the hydrodynamic interaction parameter κ as a function of the cluster size n on a double logarithmic scale. Power-law fits to the data yield the exponents b_η and b_Ψ as a function of κ (bottom).

C. Ring Polymers

We suspect that the observed variation of the exponent values with κ may be due to crossover and finite-size effects. To clarify this question it is useful to study a system where the exponents are known analytically. Therefore we (re-)investigate the viscosity η_{ring} and the first normal stress coefficient $\Psi_{\mathrm{ring}}^{(1)}$ of ring polymers in the Zimm model with the Rotne–Prager–Yamakawa tensor. The scaling of both quantities with ring size n as $n \to \infty$ can be deduced from long-

standing analytical results,[41] which lead to $b_{\eta,\mathrm{ring}} = 1/2$ and $b_{\Psi,\mathrm{ring}} = 2$. We focus here on the onset of this asymptotic behaviour and how it is affected by crossovers for different κ. This provides us with a reference system when discussing the scaling of η_n and $\Psi_n^{(1)}$ in the case of random clusters in Section V.

Due to the cyclic structure of a ring polymer the associated matrices H^{eq} and Γ are circulant matrices. Hence, they are simultaneously diagonalizable. In fact, the j-th component of the l-th eigenvector of $\widehat{\Gamma}$ for a ring of size n is explicitely given by $\psi_j^{(l)} = \exp(i2\pi jl/n)$, and as a result the eigenvalues can be written in terms of Fourier transforms.[32] Therefore, η_{ring} and $\Psi_{\mathrm{ring}}^{(1)}$ are efficiently computed by Fast Fourier Transformation up to ring sizes $n = 10^5$. The resulting viscosity and the first normal stress coefficient are shown in Figs. 2(a) and (b) on a double logarithmic scale. The data is then fitted to a power law in two different fit ranges. In addition to a fit in the terminal large-n range, $n \in [10^4, 10^5]$, we performed a second fit in the range $n \in [500, 5000]$, which is roughly where we had to do the fits in the random-cluster case. The fit exponents are shown in Fig. 2(c). Apparently, they depend on the fit range. For $\kappa = 0.05$ we find $b_{\eta,\mathrm{ring}} = 0.69$ from the small-n fit. This value clearly exceeds the theoretical one $b_{\eta,\mathrm{ring}} = 1/2$. Even the corresponding value $b_{\eta,\mathrm{ring}} = 0.58$ from the large-n fit still has an error of 36%. In contrast, for $\kappa = 0.3$ both values, $b_{\eta,\mathrm{ring}} = 0.51$ and 0.50, are quite close to the exact one.

In fact, given the Fourier representation of the eigenvalues of $\widehat{\Gamma}$, it is straightforward to demonstrate the occurrence of a crossover at $n \approx \pi/\kappa^2$ from Rouse behaviour, $\eta_{\mathrm{ring}} \sim n$, to the asymptotic Zimm behaviour $\eta_{\mathrm{ring}} \sim n^{1/2}/\kappa$ for all $n \gg \kappa^{-2}$. Hence, the larger κ, the less important is residual Rouse behaviour in the numerical data for the scaling of η_{ring}. The same holds true for $\Psi_{\mathrm{ring}}^{(1)}$. Unfortunately, choosing larger values for κ is not a practicable way out for obtaining good-quality data. This is because for large κ the asymptotics

$$h(x) \sim 1 - (\pi x)^{-1/2} \tag{34}$$

of (10) as $x \to \infty$ becomes noticible and leads to the transient behaviour $\eta_{\mathrm{ring}} \sim \kappa n^0$ for intermediate n. We have observed such a behaviour for (unphysically large) $\kappa > 10$ (not shown). But even the data for $\kappa = 0.5$ and $\kappa = 1.0$ in Fig. 2 are still slightly influenced by (34).

In summary, whereas there is a generic overestimate of the scaling exponents for small κ due to residual Rouse behaviour, the exponents are underestimated for higher κ due to the asymptotics (34). The optimal value for minimal finite-size effects in ring polymers appears to be $\kappa \approx 0.3$ in Fig. 2(c).

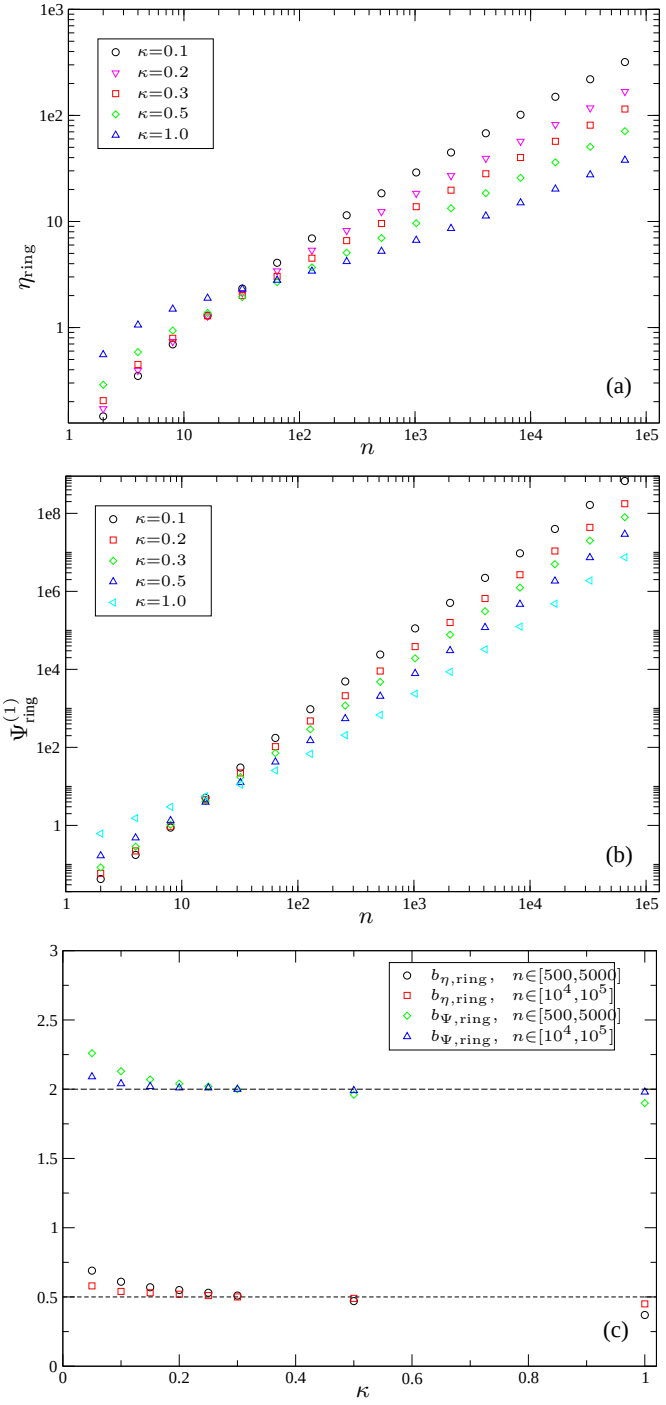

FIG. 2: Numerical data to determine the scaling (33) for ring polymers. The viscosity η_{ring} (a) and the normal stress coefficient $\Psi_{\mathrm{ring}}^{(1)}$ (b) are plotted for different strengths of the hydrodynamic interaction parameter κ as a function of the cluster size n on a double logarithmic scale. (c) shows the exponents $b_{\eta,\mathrm{ring}}$ and $b_{\Psi,\mathrm{ring}}$ from power-law fits to the data of (a) and (b). The fits were performed for two different ranges of cluster sizes n. Additional data points for $\kappa = 0.05, 0.15$ and 0.25 in (c) stem from curves which have been omitted in (a) and (b) for reasons of clarity. The two horizontal lines indicate the exact values $b_{\eta,\mathrm{ring}} = 1/2$ and $b_{\Psi,\mathrm{ring}} = 2$.

V. DISCUSSION

Using the Zimm model for randomly crosslinked monomers, we have determined the scaling (33) of the averaged viscosity and of the averaged first normal stress coefficient over clusters of a given size n. Figs. 1(c) and (f) display a crossover from the Rouse values at $\kappa = 0$ to the Zimm values at non-zero κ. We estimate the latter as

$$b_\eta \approx 0.11 \qquad \text{and} \qquad b_\Psi \approx 0.77\,, \tag{35}$$

from our data for $\kappa = 0.3$. A detailed discussion of this choice of κ and of possible origins of the dependence of b_η and b_Ψ on κ will be given below. Within the accuracy of our data, the exponents are the same for both Erdős–Rényi random graphs and three-dimensional percolation.

The critical behaviour of the averaged viscosity $\langle\eta\rangle \sim \varepsilon^{-k}$ and of the averaged first normal stress coefficient $\langle\Psi^{(1)}\rangle \sim \varepsilon^{-\ell}$ for a polydisperse gelling solution of crosslinked monomers then follows from (35) and (32). For the viscosity this implies a *finite* value at the gel point for both, Erdős–Rényi random graphs and three-dimensional bond percolation. In contrast, the first normal stress coefficient is found to diverge with an exponent that depends on the cluster statistics. Choosing the cluster statistics according to Erdős–Rényi random graphs, we find $\ell \approx 0.54$. The case of three-dimensional bond percolation leads to the higher value $\ell \approx 1.3$. These exponent values are less than a third in magnitude than the corresponding exact analytical predictions $\ell = 3$, respectively $\ell \approx 4.1$ of the Rouse model for randomly crosslinked monomers[4,5,6] with the corresponding cluster statistics.

The dependence of the critical exponents b_η and b_Ψ on the hydrodynamic interaction strength κ in Figs. 1(c) and (f) may be due to finite-size effects. In particular the onset of the true asymptotic regime of these quantities may depend on κ. In order to better understand finite-size effects, we have examined the Zimm dynamics of polymer rings in Sec. IV C and determined the scaling of the viscosity $\eta_{\text{ring}} \sim n^{b_{\eta,\text{ring}}}$ and of the first normal stress coefficient $\Psi^{(1)}_{\text{ring}} \sim n^{b_{\Psi,\text{ring}}}$ with the ring size n. For rings one can access much higher values of n as for random clusters, see Figs. 2(a) and (b). In particular, the exactly known scaling exponents $b_{\eta,\text{ring}} = 1/2$ and $b_{\Psi,\text{ring}} = 2$, which are universal in $\kappa > 0$, can be extracted from our data in Fig. 2(c). However, if we did not exploit the full range of available ring sizes and restricted the fit to those lower values of n which could also be accessed for random clusters, then universality would be veiled by finite-size effects. Finite-size effects are more pronounced for $\kappa \leq 0.15$ and $\kappa > 0.5$. Thus, we conclude (i) that the random-cluster data have not reached either the asymptotic large-n regime yet for $\kappa \leq 0.15$ in Fig. 1, (ii) that the asymptotic regime *is* universal and (iii) that the data for $\kappa = 0.3$ should be the most reliable ones.

The exponent b_η has also been investigated experimentally. In Ref. 42 measurements on randomly branched polystyrenes have been performed, resulting in $b_\eta \in [0.2, 0.25]$. Measurements on branched polyethyleneimine[43] yield the slightly higher value $b_\eta \approx 0.31$. Brownian-dynamics simulations of hyperbranched polymers were performed in Ref. 44. They also account for *fluctuating* hydrodynamic interactions corresponding to $\kappa = 0.35$, as well as for excluded-volume interactions and lead to $b_\eta = 0.13$. This result is remarkably close to our finding $b_\eta \approx 0.11$ for the highest coupling strength $\kappa = 0.3$ that we have considered, whereas the experimental findings are consistently above our value (see the discussion below).

Next we compare our findings with the scaling argument which is summarized in Eq. (1). For phantom clusters, *i.e.* in the absence of excluded-volume interactions, the Hausdorff fractal dimension is equal to the Gaussian fractal dimension[18,45] $d_f^{(\text{G})} := 2d_s/(2 - d_s)$, where d_s is the spectral dimension. Here we estimate $d_s \approx 4/3$ according to the Alexander–Orbach conjecture, which is known to be an excellent approximation albeit not being exact. For $d = 3$ Eq. (1) then implies $b_\eta \approx -1/4$, and for $d = 6$ one has $b_\eta \approx 1/2$. The latter value corresponds to Erdős–Rényi random graphs, whose critical properties are identical to those of mean-field percolation.[37] Both values can be definitely ruled out by our data. Thus we conclude that the scaling relation (1) does not apply to the Zimm model for randomly crosslinked monomers. This failure comes as a surprise because it is known from a recent investigation of diffusion constants within this model[19] that the exact results are in accordance with long standing scaling relations when inserting $d_f^{(\text{G})}$ for d_f.

Coming back to the experimental k-values listed in Table I and considering also the exact prediction $k = (1 - \tau + 2/d_s)/\sigma \approx 0.71$ of the Rouse model for gelling monomers,[2,3,6] we conclude that an explanation for the broad scatter of the data in the literature calls for additional relevant interactions than those accounted for in the Zimm or Rouse model. This may be due to the preaveraging approximation. In particular, it throws away hydrodynamic interactions among different clusters. But we do not expect this to be the sole relevant simplification of the Zimm model, because linear polymers show a decrease in the viscosity when abandoning the preaveraging approximation,[46] and effects of preaveraging for branched molecules are even more pronounced than those for linear ones.[47] Rather it seems that there are no satisfactory explanations without considering excluded-volume interactions. Indeed, simulations[48] of the bond-fluctuation model deliver higher values $k \approx 1.3$ in accordance with the scaling relation $k = 2\nu - \beta$, which arises from heuristically merging Rouse-type and excluded-volume properties.

Acknowledgments

We acknowledge financial support by the DFG through SFB 602 and Grant No. Zi 209/6–1.

* Electronic address: loewe@theorie.physik.uni-goettingen.de
† Electronic address: mueller@theorie.physik.uni-goettingen.de
‡ Electronic address: zippelius@theorie.physik.uni-goettingen.de

[1] P. E. Rouse, J. Chem. Phys. **21**, 1272 (1953).
[2] K. Broderix, H. Löwe, P. Müller, and A. Zippelius, Europhys. Lett. **48**, 421 (1999).
[3] K. Broderix, H. Löwe, P. Müller, and A. Zippelius, Phys. Rev. E **63**, 011510 (2001).
[4] K. Broderix, H. Löwe, P. Müller, and A. Zippelius, Physica A **02**, 279 (2001).
[5] K. Broderix, P. Müller, and A. Zippelius, Phys. Rev. E **65**, 041505 (2002).
[6] P. Müller, J. Phys. A **36**, 10443 (2003).
[7] B. H. Zimm, J. Chem. Phys. **24**, 269 (1956).
[8] T. Takigawa, K. Urayama, and T. Masuda, J. Chem. Phys. **93**, 7310 (1990).
[9] M. Adam, M. Delsanti, R. Okasha, and G. Hild, J. Phys. (Paris) Lett. **40**, L-539 (1979).
[10] M. A. V. Axelos and M. Kolb, Phys. Rev. Lett. **64**, 1457 (1990).
[11] J. Dumas and J.-C. Bacri, J. Phys. (Paris) Lett. **41**, L-279 (1980).
[12] H. Zheng, Q. Zhang, K. Jiang, H. Zhang, and J. Wang, J. Chem. Phys. **105**, 7746 (1996).
[13] C. P. Lusignan, T. H. Mourey, J. C. Wilson, and R. H. Colby, Phys. Rev. E **52**, 6271 (1995).
[14] R. H. Colby, J. R. Gillmor, and M. Rubinstein, Phys. Rev. E **48**, 3712 (1993).
[15] C. P. Lusignan, T. H. Mourey, J. C. Wilson, and R. H. Colby, Phys. Rev. E **60**, 5657 (1999).
[16] D. Stauffer, A. Coniglio, and M. Adam, Adv. in Polym. Sci. **44**, 103 (1982).
[17] M. Muthukumar, J. Chem. Phys. **83**, 3161 (1985).
[18] M. E. Cates, J. Physique (France) **46**, 1059 (1985).
[19] M. Küntzel, H. Löwe, P. Müller, and A. Zippelius, Eur. Phys. J. E **12**, 325 (2003).
[20] B. H. Zimm and R. W. Kilb, J. Pol. Sci., Part B, Polymer Physics Ed. **34**, 1367 (1996).
[21] C. von Ferber and A. Blumen, J. Chem. Phys. **116**, 8616 (2002).
[22] A. Jurjiu, T. Koslowski, and A. Blumen, J. Chem. Phys. **118**, 2398 (2003).
[23] M. Plischke, D. C. Vernon, and Béla Joós, Phys. Rev. E **67**, 011401 (2003).
[24] M. Doi and S. F. Edwards, *The Theory of Polymer Dynamics* (Clarendon Press, Oxford 1988).
[25] R. B. Bird, C. F. Curtiss, R. C. Armstrong, and O. Hassager, *Dynamics of Polymeric Liquids*, vol. 2 (Wiley, New York 1987).
[26] C. W. Oseen, Ark. Mat. Astr. Fys. **6**, No. 29, 1 (1910).
[27] J. G. Kirkwood and J. Riseman, J. Chem. Phys. **16**, 565 (1948).
[28] P. Erdős and A. Rényi, Magyar Tud. Akad. Mat. Kut. Int. Kőzl **5**, 17 (1960); reprinted in: *P. Erdős: the Art of Counting*, ed. J. Spencer (MIT Press, Cambridge, MA 1973), Chap. 14, Article 324.
[29] D. Stauffer and A. Aharony, *Introduction to Percolation Theory* (Taylor and Francis, London 1994).
[30] A. E. Albert, *Regression and the Moore–Penrose pseudoinverse* (Academic Press, New York 1972).
[31] D. J. Klein and M. Randìc, J. Math. Chem **12**, 81 (1993).
[32] H. C. Öttinger and W. Zylka, J. Rheol. **36**, 885 (1992).
[33] K. Broderix, P. M. Goldbart, and A. Zippelius, Phys. Rev. Lett. **79**, 3688 (1997).
[34] J. Rotne and S. Prager, J. Chem. Phys. **50**, 4831 (1969).
[35] H. Yamakawa, J. Chem. Phys. **53**, 436 (1970).
[36] M. Fixman, J. Chem. Phys. **78**, 1594 (1983).
[37] M. J. Stephen, Phys. Rev. B **15**, 5674 (1977).
[38] K. Mehlhorn and S. Näher, *LEDA – A Platform for Combinatorial and Geometrical Computing* (Cambridge University Press, Cambridge 1999).
[39] P. L. Leath, Phys. Rev. B **14**, 5046 (1976).
[40] M. F. Sykes, D. S. Gaunt, and M. Glen, J. Phys. A **14**, 287 (1981).
[41] V. Bloomfield and B. H. Zimm, J. Chem. Phys. **44**, 315 (1966).
[42] T. Masuda, Y. Ohta, and S. Onogi, Macromolecules **19**, 2524 (1986).
[43] I. H. Park and E-J. Choi, Polymer **37**, 313 (1996).
[44] P. F. Sheridan, D. B. Adolf, A. V. Lyulin, I. Neelov, and G. R. Davies, J. Chem. Phys. **117**, 7802 (2002).
[45] T. A. Vilgis, Physica A **153**, 341 (1988).
[46] M. Fixman, Macromolecules **14**, 1710 (1981).
[47] W. Burchard, M. Schmidt, and W. H. Stockmayer, Macromolecules **13**, 580 (1980).
[48] E. Del Gado, L. de Arcangelis, and A. Coniglio, Eur. Phys. J. E **2**, 359 (2000).